SUPPORTING INFORMATION

Solution and Solid-state Properties of Highly Fluorescent Dithieno[3,2-*b*:2',3'-*d*]pyrrole-based Oligothiophenes

Hong Mo, Karla R. Radke, Katsu Ogawa, Christopher L. Heth, Brett T. Erpelding, and Seth C. Rasmussen*

Department of Chemistry and Biochemistry, North Dakota State University, NDSU Dept. 2735, P.O. Box 6050, Fargo, ND 58108-6050, USA. Fax: 1-701-231-8747; Tel: 1-701-231-8831; E-mail: seth.rasmussen@ndsu.edu

Table of Contents:

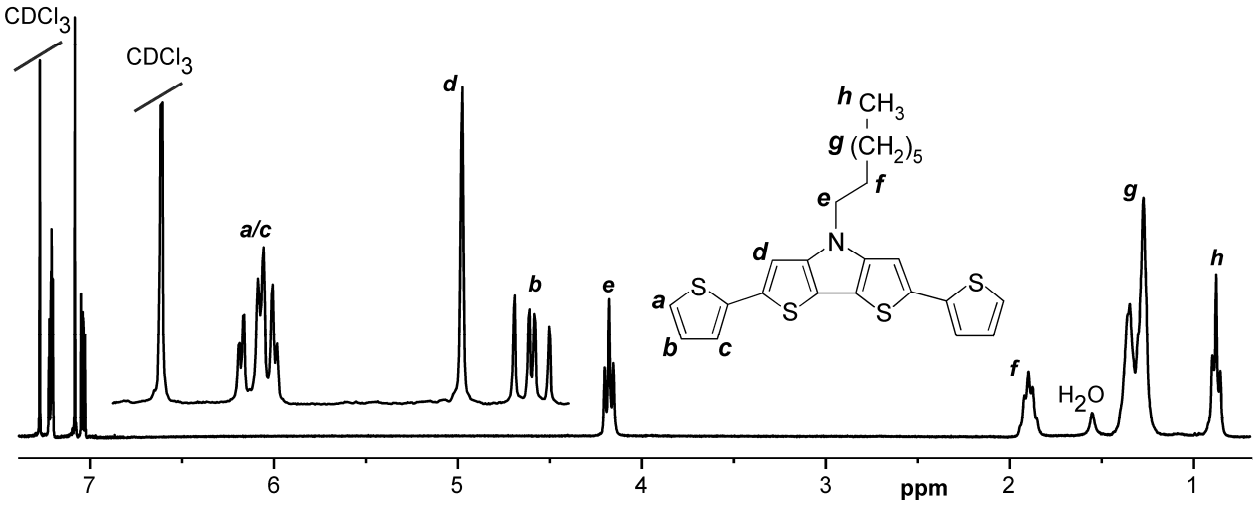

Figure S1. [1]H NMR Spectrum of Compound **8a**

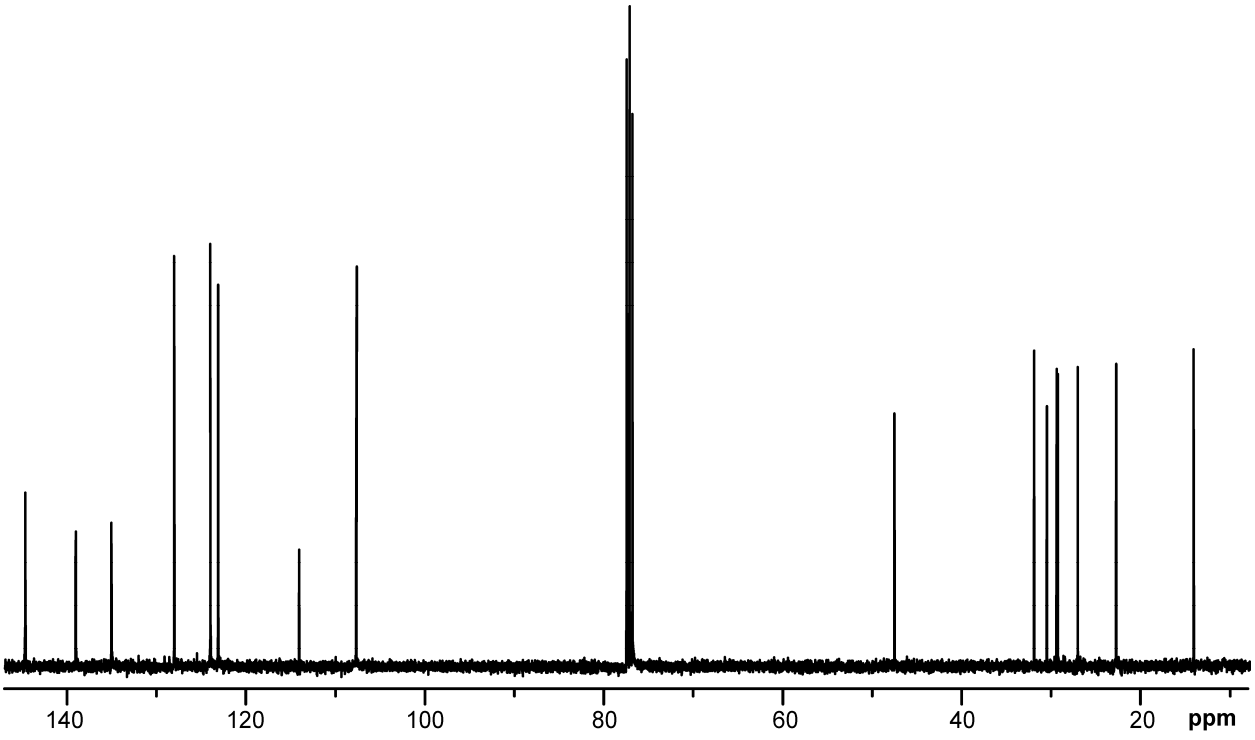

Figure S2. [13]C NMR Spectrum of Compound **8a**

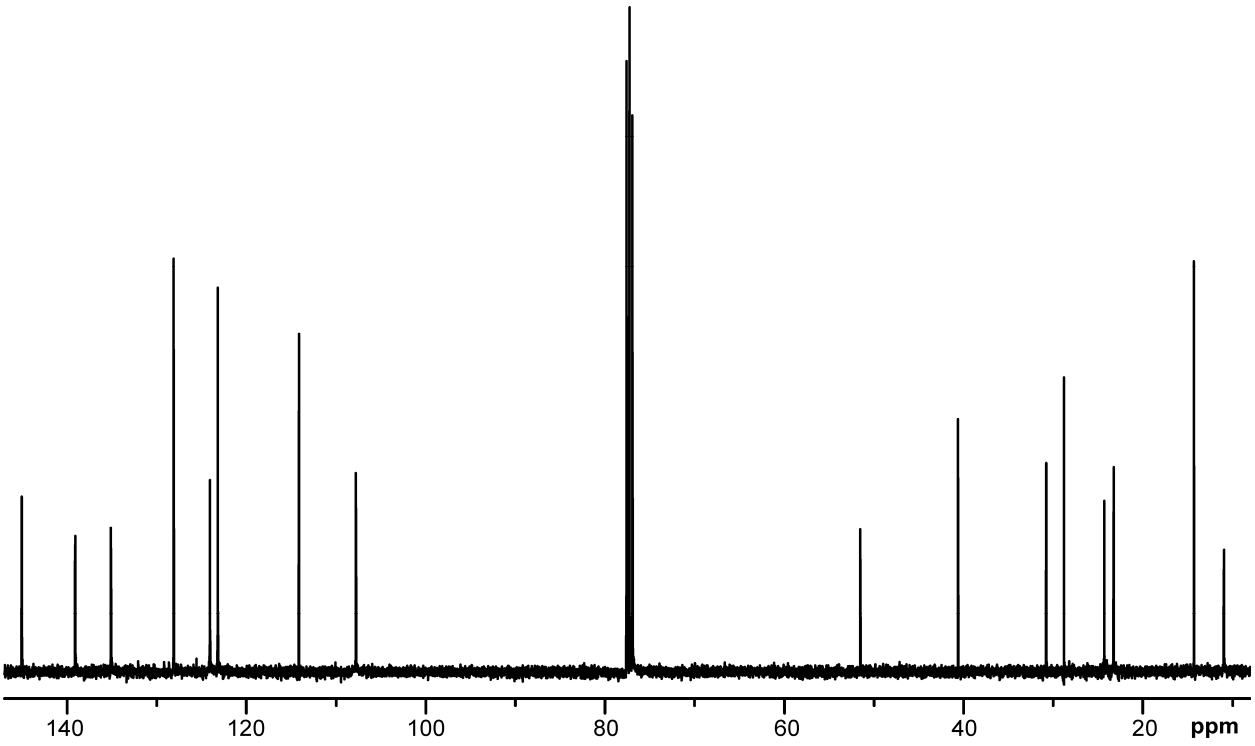

Figure S3. ^{13}C NMR Spectrum of Compound **8b**

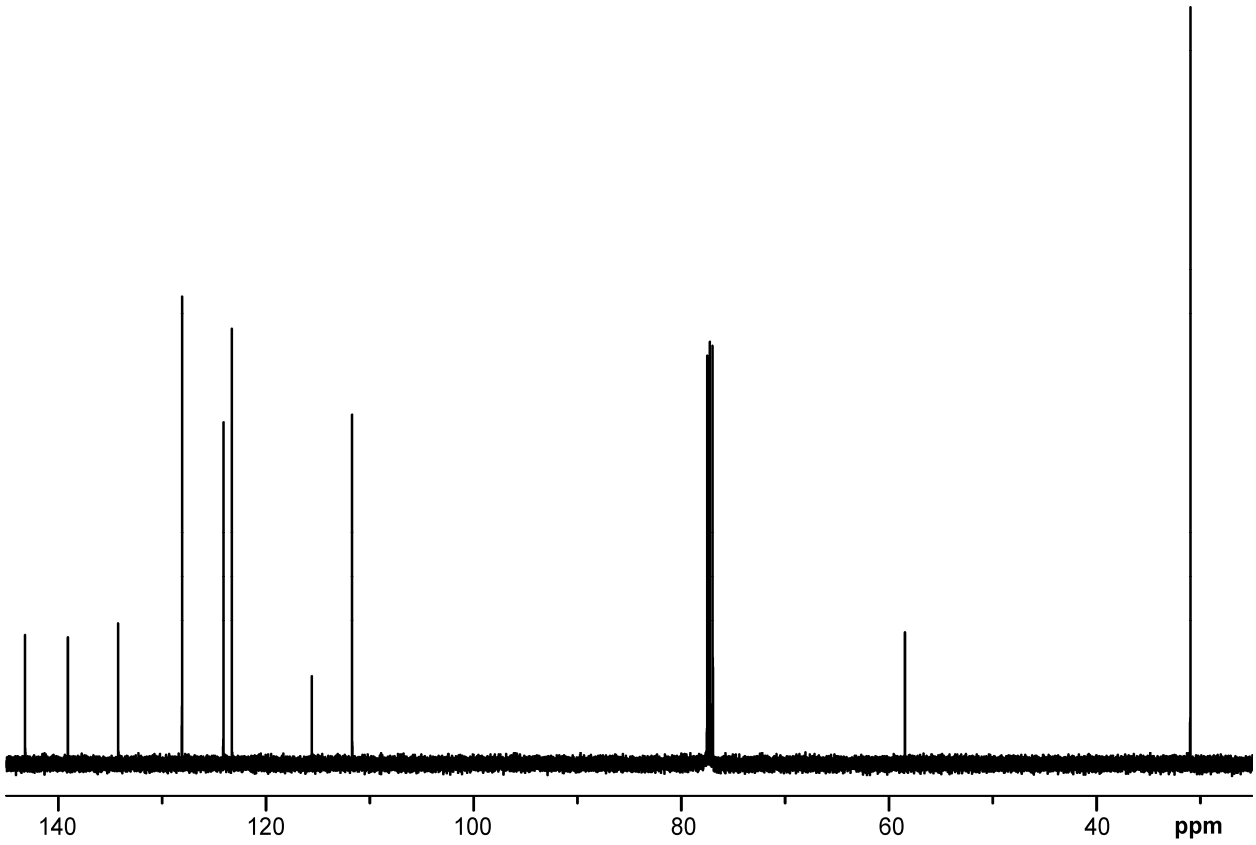

Figure S4. ^{13}C NMR Spectrum of Compound **8c**

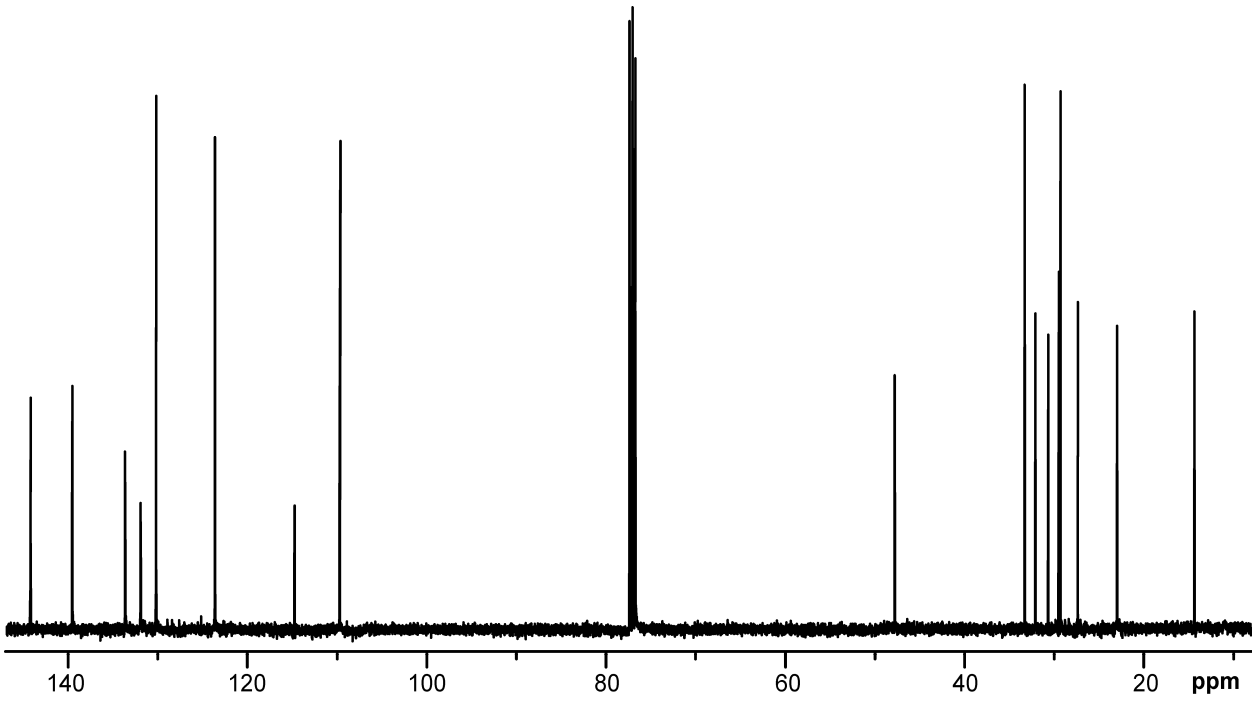

Figure S5. ^{13}C NMR Spectrum of Compound **8d**

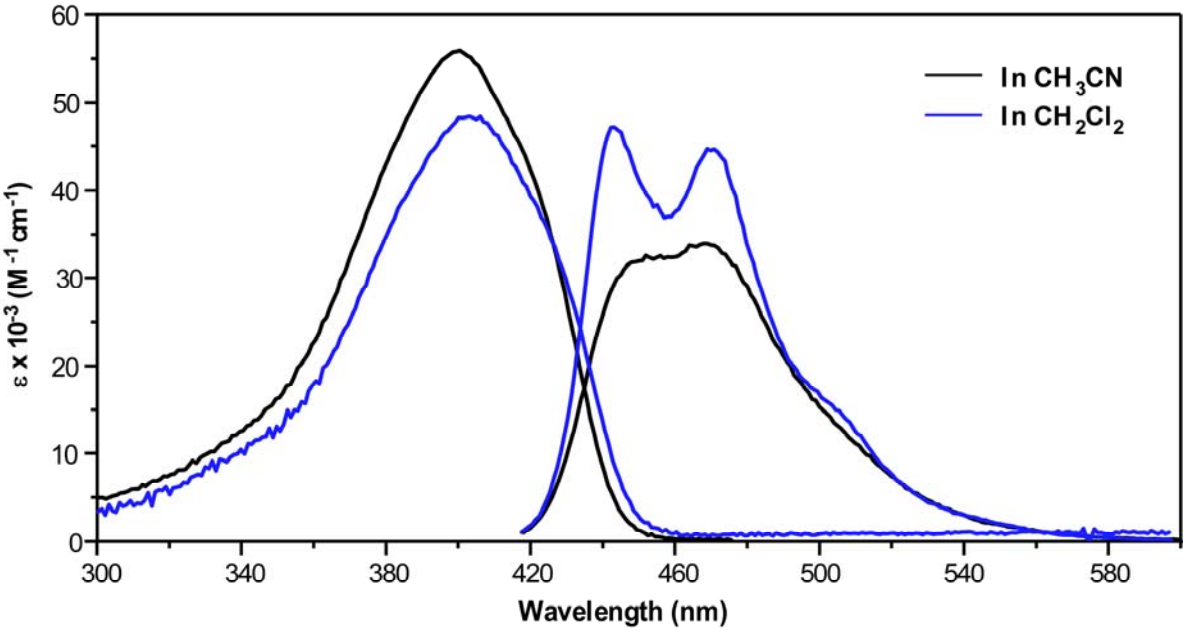

Figure S6. Absorption and Emission spectra of Compound **8a** in CH_3CN and CH_2Cl_2

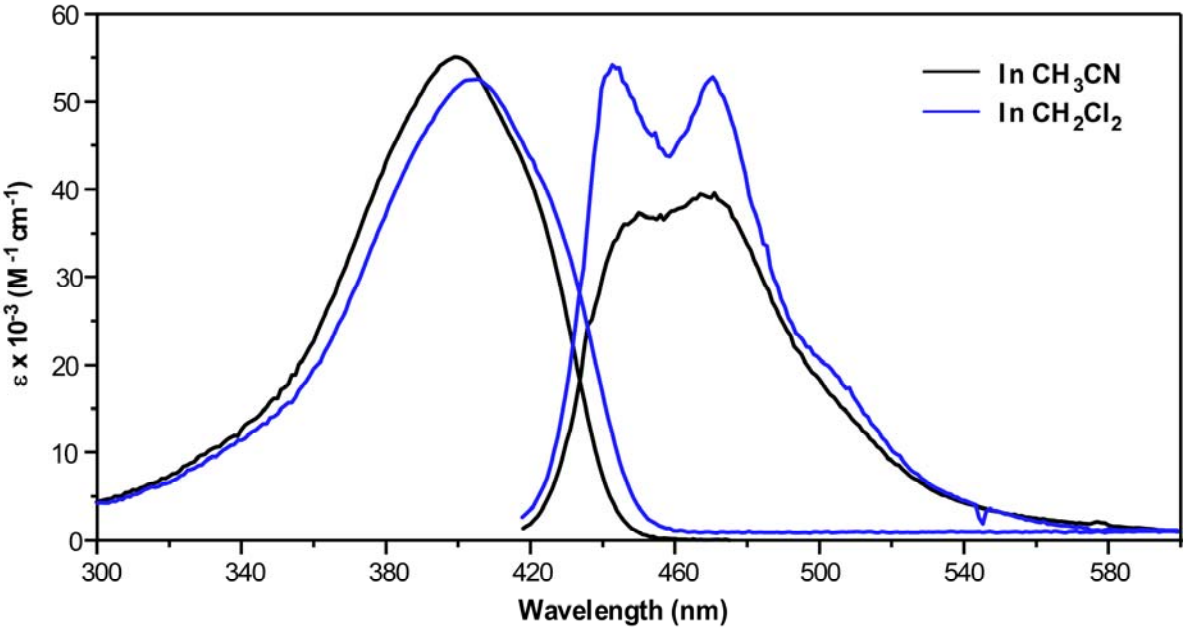

Figure S7. Absorption and Emission spectra of Compound **8b** in CH_3CN and CH_2Cl_2

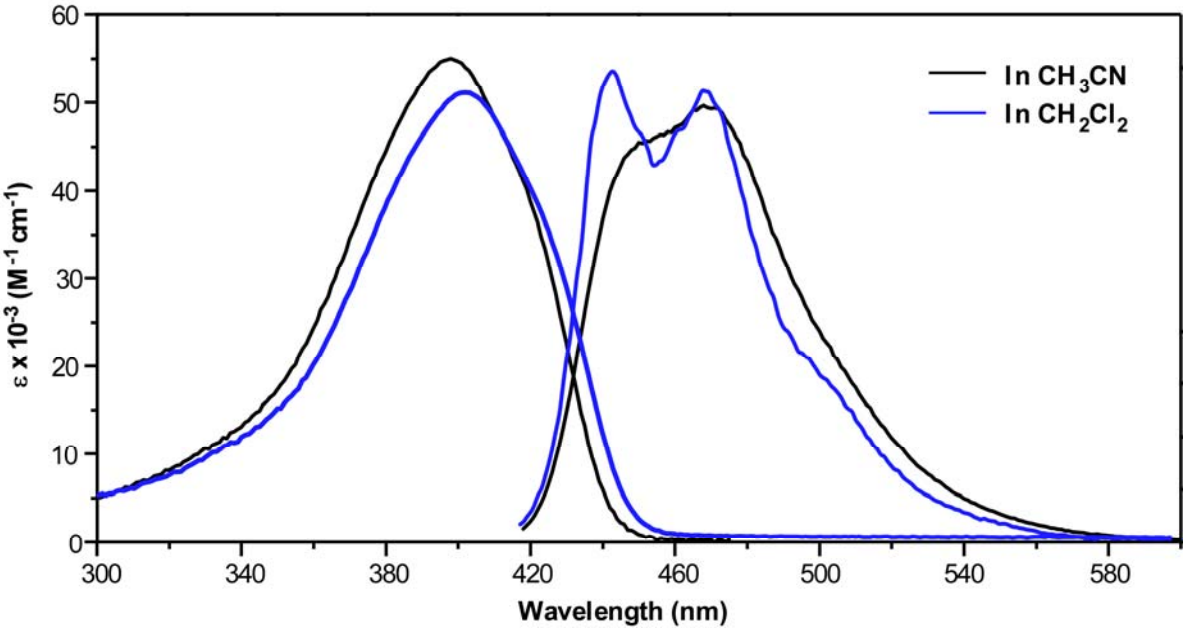

Figure S8. Absorption and Emission spectra of Compound **8c** in CH_3CN and CH_2Cl_2

X-ray Crystallography. X-ray quality crystals of **8c** were grown by the slow evaporation of toluene solutions. The X-ray intensity data of the crystals were measured at 298 K on a Bruker SMART 1000 CCD-based X-ray diffractometer system equipped with a Mo-target X-ray tube (λ = 0.71073 Å) operated at 2000 W of power. The detector was placed at a distance of 5.047 cm from the crystal. A total of 1321 frames were collected with a scan width of 0.3° in ω and exposure time of 10 s/frame. The total data collection time was 7 h. The frames were integrated with the Bruker SAINT software package using an arrow-frame integration algorithm. All data were integrated using a monolinic unit cell and the structure was refined using the Bruker SHELXTL (Version 5.1) Software Package. The crystal data, data collection parameters, and refinement statistics are listed in Table S1. Full crystallography data for compound is attached as a separate CIF file.

Table S1. Crystal data, data collection parameters, and refinement statistics for **8c**

Formula	$C_{20}H_{17}NS_4$	Z	4
Formula Weight	399.59	d_{calc} (g cm^{-3})	1.395
Temperature (K)	293(2)	μ (mm^{-1})	0.502
Crystal System	monoclinic	Reflections collected	37314
Space Group	$P2_1/c$	Unique reflections	4247 [R_{int} = 0.0939]
a (Å)	17.489(4)	Observed reflections	2227
b (Å)	7.8855(16)	Final R indices [$I>2\sigma(I)$]	R_1 = 0.0386
c (Å)	14.540(3)		wR_2 = 0.0814
α (º)	90.00	R indices (all data)[a]	R_1 = 0.1027
β (º)	108.37(3)		wR_2 = 0.0877
γ (º)	90.00	Goodness-of-fit on F^2	1.003
V (Å^3)	1903.0(8)		

[a] $R_1 = \Sigma(||F_o| - |F_c||) / \Sigma|F_o|$, $wR_2 = [\Sigma(w(F_o^2 - F_c^2)^2) / \Sigma(F_o^2)^2]^{1/2}$, Goodness-of-fit on F^2 = $[\Sigma(w(F_o^2 - F_c^2)^2 / (n-p)]^{1/2}$, where n is the number of reflections and p is the number of parameters refined.

Thin film diffraction. The x-ray diffraction characterization of spun-cast thin films of **8c** was collected on a Philips MPD (Multi-Purpose Diffractometer) using graphite-monochromated Cu $K\alpha$ radiation (λ = 1.54056 Å). The patterns were collected between 4 and 70º (2θ), with a step size of 0.02 and counting 2 s per step. For comparison, the powder diffraction pattern was calculated from the single crystal data using the Mercury software package (ver.1.4.1, CCDC) and the overlaid patterns are shown in Figure S6.

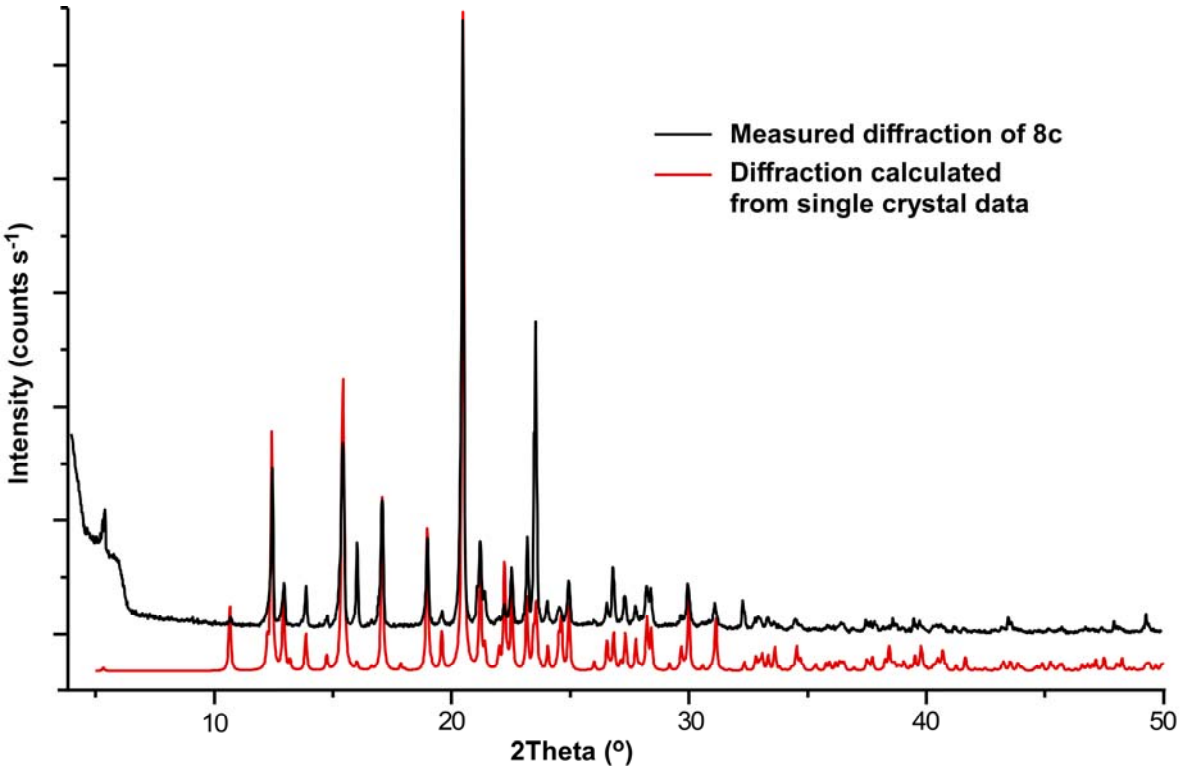

Figure S6. Measured and calculated diffraction patterns for thin films of oligomer **8c**.

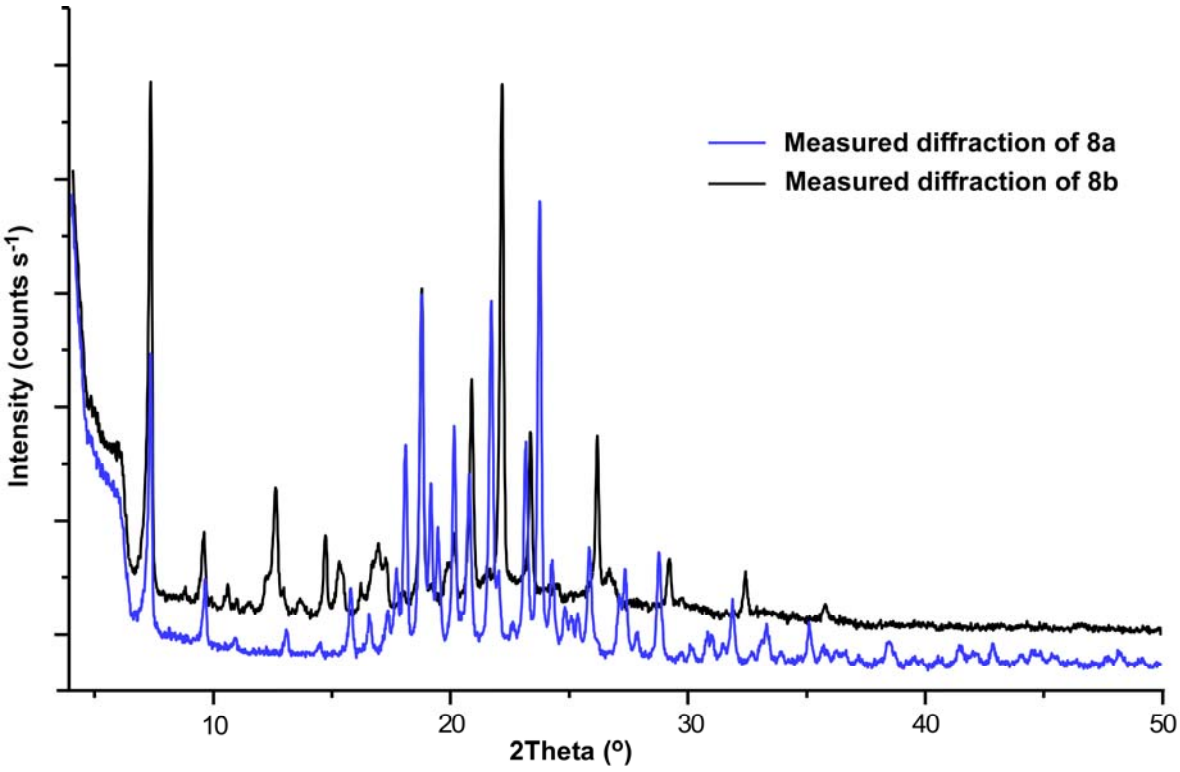

Figure S7. Measured diffraction patterns for thin films of oligomers **8a** and **8b**.

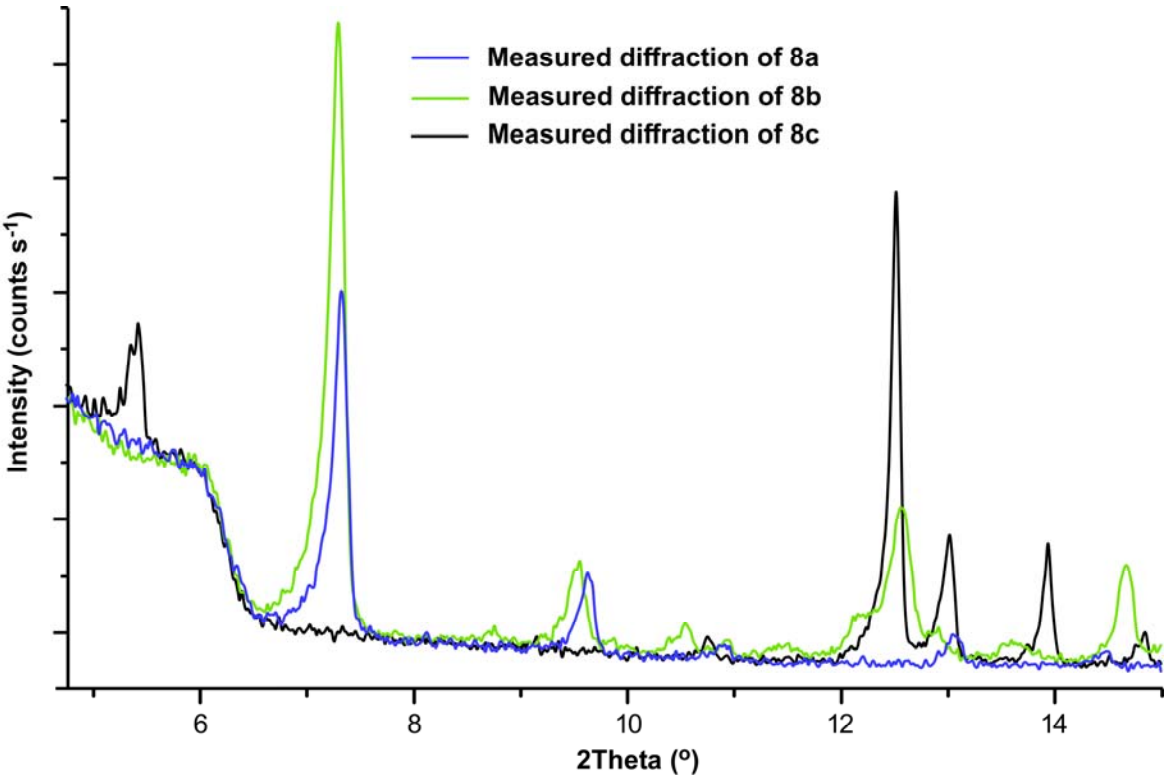

Figure S8. Low angle diffraction region for thin films of oligomers **8a-c**.

Computational Modeling. Calculations were performed using the Gaussian 03 software package.[1] Optimized geometries were calculated using DFT methods, a B3LYP correlation functional, and a 6-31G* basis set with the geometric parameters of the interior pyrrole ring (where appropriate) constrained to values determined from experimental crystal structures. Single point energy calculations using methods matching the geometry optimization were then performed, followed by ZINDO calculations. In all calculations, molecular symmetry was ignored and SCF convergence criteria were set to "very tight". While the use of Hartree-Fock methods for the single point calculation had no effect on the ZINDO results, use of Hartree-Fock methods to optimize the geometry resulted in a reordering of some molecular orbitals and ZINDO results less in line with experiment. Molecular orbital diagrams were generated using GaussView 3.09 from the checkpoint file generated during the single point energy calculation and a 0.022 isovalue.

Table S2. Experimental and Calculated Geometric Parameters of DTP-based Quaterthiophenes **8a-c**.

Parameter	8c	8c (calc)	8b (calc)	8a (calc)
S(3)-C(1)	1.583(3)	1.7368	1.7366	1.7367
S(3)-C(4)	1.607(2)	1.7589	1.7587	1.7587
C(1)-C(2)	1.337(3)	1.3673	1.3675	1.3675
C(2)-C(3)	1.605(3)	1.4239	1.4237	1.4236
C(3)-C(4)	1.643(2)	1.3795	1.3796	1.3796
C(4)-C(5)	1.467(3)	1.4468	1.4463	1.4464
S(1)-C(5)	1.744(2)	1.7735	1.7799	1.7797
S(1)-C(8)	1.720(2)	1.7372	1.7400	1.7402
C(5)-C(6)	1.359(3)	1.3797	1.3809	1.3808
C(6)-C(7)	1.419(3)	1.4244	1.4166	1.4166
C(7)-C(8)	1.394(3)	1.4083	1.4056	1.4060
C(8)-C(9)	1.407(3)	1.4028	1.4087	1.4088
N(1)-C(7)	1.400(2)	1.390	1.3861	1.3864
S(4)-C(16)	1.651(3)	1.7368	1.7366	1.7366
S(4)-C(13)	1.683(2)	1.7589	1.7587	1.7587
C(16)-C(15)	1.330(3)	1.3674	1.3675	1.3675
C(15)-C(14)	1.462(3)	1.4238	1.4237	1.4237
C(14)-C(13)	1.494(3)	1.3796	1.3796	1.3796
C(13)-C(12)	1.452(3)	1.4465	1.4463	1.4463
C(1)-S(3)-C(4)	95.35(15)	91.83	91.82	91.82
S(3)-C(1)-C(2)	116.8(2)	111.54	111.55	111.55
C(1)-C(2)-C(3)	116.8(2)	113.01	113.01	113.00
C(2)-C(3)-C(4)	93.79(14)	113.63	113.61	113.61
S(3)-C(4)-C(5)	120.98(17)	121.02	120.93	120.95
C(5)-S(1)-C(8)	90.77(10)	90.48	90.83	90.83
S(1)-C(5)-C(6)	112.83(16)	112.21	112.10	112.10
S(1)-C(8)-C(7)	111.72(15)	112.24	111.01	111.00
C(5)-C(6)-C(7)	111.97(18)	112.60	111.88	111.88
C(6)-C(7)-C(8)	112.71(17)	112.47	114.18	114.21
C(7)-N(1)-C(10)	106.54(15)	106.33	106.80	106.86
N(1)-C(7)-C(8)	109.14(17)	109.28	109.68	109.65
C(7)-C(8)-C(9)	107.42(17)	107.48	106.91	106.91
C(16)-S(4)-C(13)	93.63(13)	91.83	91.83	91.83
S(4)-C(16)-C(15)	113.50(19)	111.54	111.56	111.55
C(16)-C(15)-C(14)	116.2(2)	113.01	113.00	113.00
C(15)-C(14)-C(13)	104.29(17)	113.63	113.61	113.61
S(4)-C(13)-C(12)	121.74(17)	120.99	120.92	120.95
C(12)-S(2)-C(9)	91.12(10)	90.60	90.87	90.88
S(1)-C(5)-C(4)-S(3)	144.15	159.88	159.54	159.24
S(2)-C(12)-C(13)-S(4)	155.57	159.82	159.35	160.74

References

1. Gaussian 03, Revision C.02, Frisch, M. J.; Trucks, G. W.; Schlegel, H. B.; Scuseria, G. E.; Robb, M. A.; Cheeseman, J. R.; Montgomery, Jr., J. A.; Vreven, T.; Kudin, K. N.; Burant, J. C.; Millam, J. M.; Iyengar, S. S.; Tomasi, J.; Barone, V.; Mennucci, B.; Cossi, M.; Scalmani, G.; Rega, N.; Petersson, G. A.; Nakatsuji, H.; Hada, M.; Ehara, M.; Toyota, K.; Fukuda, R.; Hasegawa, J.; Ishida, M.; Nakajima, T.; Honda, Y.; Kitao, O.; Nakai, H.; Klene, M.; Li, X.; Knox, J. E.; Hratchian, H. P.; Cross, J. B.; Bakken, V.; Adamo, C.; Jaramillo, J.; Gomperts, R.; Stratmann, R. E.; Yazyev, O.; Austin, A. J.; Cammi, R.; Pomelli, C.; Ochterski, J. W.; Ayala, P. Y.; Morokuma, K.; Voth, G. A.; Salvador, P.; Dannenberg, J. J.; Zakrzewski, V. G.; Dapprich, S.; Daniels, A. D.; Strain, M. C.; Farkas, O.; Malick, D. K.; Rabuck, A. D.; Raghavachari, K.; Foresman, J. B.; Ortiz, J. V.; Cui, Q.; Baboul, A. G.; Clifford, S.; Cioslowski, J.; Stefanov, B. B.; Liu, G.; Liashenko, A.; Piskorz, P.; Komaromi, I.; Martin, R. L.; Fox, D. J.; Keith, T.; Al-Laham, M. A.; Peng, C. Y.; Nanayakkara, A.; Challacombe, M.; Gill, P. M. W.; Johnson, B.; Chen, W.; Wong, M. W.; Gonzalez, C.; and Pople, J. A.; Gaussian, Inc., Wallingford CT, 2004.